Available online www.jsaer.com

***Journal of Scientific and Engineering Research*, 2018, 5(10):241-251**

Research Article

ISSN: 2394-2630
CODEN(USA): JSERBR

Influence of Both Magnetic Field and Temperature on Silicon Solar Cell Photogenerated Current

Richard Mané[1], Hawa Ly Diallo[1], Hameth yoro BA[2], Ibrahima Diatta[1], Youssou Traoré[1], Cheikh Tidiane Sarr[1], Grégoire Sissoko[1]

[1]Laboratoire des Semi-conducteurs et d'Energie Solaire, Faculté des Sciences et Techniques, Université Cheikh Anta Diop, Dakar, Sénégal
[2]Ecole Polytechnique de Thiès, Sénégal

Abstract In this work, we propose a study of the silicon solar cell under magnetic field in the presence of temperature. The object of this study is the determination of the short-circuit photocurrent for different temperature values corresponding to a maximum diffusion of the minority charge carriers. These temperature values, called Topt (B), are a function of the magnetic field and are obtained from the evolution of the diffusion coefficient of the minority charge carriers as a function of the temperature for different values of the magnetic field. These optimal temperature values Topt (B) will allow the study of the minority charge carriers density and the photocurrent.

Keywords Silicon Solar Cell, Photocurrent, Temperature, Magnetic field

1. Introduction

The quality of a solar cell is closely linked to its electronic parameters which depend on the diffusion coefficient and to its electrical parameters, the increase of which will influence the efficiency of the photovoltaic array [1-2]. Among these electrical parameters, one can cite the photocurrent [3-5]. The latter characterizes the flow of electrons passing through the junction and therefore the performance of the solar cell [6-8]. Several parameters influence the photocurrent [9], which explains its record 25.6% efficiency for silicon solar cells [10]. Thus, several characterization techniques, including the effect of the magnetic field [3, 11, 12], the electric field [13], the doping rate [14], the temperature [15,16] recombination at the grain boundaries [17], the grain size [17], the recombination velocity at the junction [18,19], the illumination level [20-23] with a solution to realize an automation orientation system of solar sensors that can be used for photovoltaic panels [24], wavelength [25], frequency [26], irradiation [27-29], the thickness of the base [30], the recombination velocity at the back [31], the recombination rate at the surface [32] and the number of junctions [33] been presented. The study of these external parameters as internal on the photocurrent was made on arbitrary choices. In our study, we consider temperatures which give a maximum diffusion of the charge minority carriers photogenerated in the base. These temperature values, called Topt (B), are a function of the magnetic field B and are obtained from the evolution of the diffusion coefficient of the minority charge carriers as a function of the temperature for different values of the magnetic field. Thus, the study of the minority charge carriers density is proposed, which will allow to access to the photocurrent.

2. Theory

In this study we consider a type of solar cell n^+-p-p^+ under polychromatic illumination. The structure of this solar cell is shown in Figure 1:

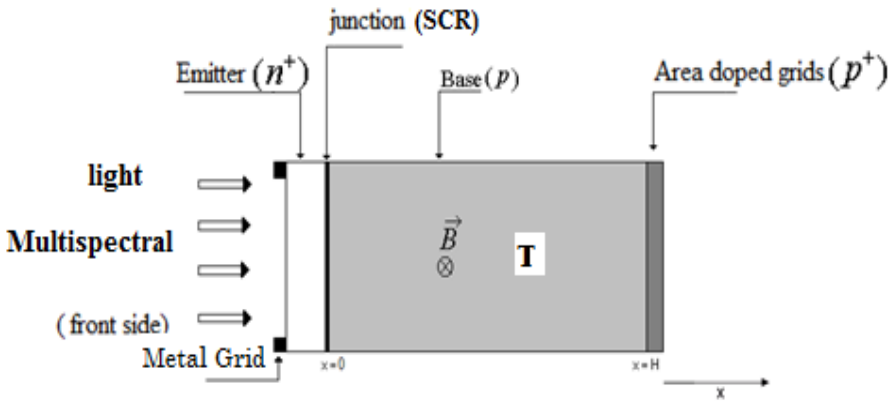

Figure 1: Silicon solar cell n+pp+ type

When the solar cell is illuminated by multispectral light various phenomena such as the creation of electron-hole pairs, the diffusion of the minority charge carriers in the base as well as the recombination can occur. The whole of these phenomena is governed by an equation called: continuity equation which is relative to the density of excess minority carriers in the base. It is represented by Equation 1:

$$\frac{\partial^2 \delta(x,B,T)}{\partial x^2} - \frac{\delta(x,B,T)}{L(B,T)^{*2}} = -\frac{G(x)}{D(B,T)^*} \quad (1)$$

G(x) represents the rate of generation of the minority load carriers which depends on the depth in the base according to relation [34]:

$$G(x) = \sum_{i=1}^{3} a_i . e^{-b_i x} \quad (2)$$

The coefficients ai and bi are obtained from the tabulated values of the radiation under $A.M_{1.5}$ [35]. These coefficients are given by:

a_1=6,13.10^{20} cm^{-3}/s; a_2=0,54.$10^{20}cm^{-3}/s$; a_3=0,0991.$10^{20}cm^{-3}/s$; b_1=6630cm^{-1}; b_2=1000cm^{-1};

D * (B, T) represents the diffusion coefficient of the minority carriers of charge in the base. It depends on the temperature and the magnetic field according to relation [4]:

$$D^*(B,T) = \frac{D_0(T)}{\left[1 + (\mu(T) \times B)^2\right]} \quad (3)$$

D0 (T) is the diffusion coefficient that is a function of temperature T in the absence of a magnetic field, given by the Einstein-Smoluchowski relation [14,15]:

$$D_0(T) = \mu(T) \times \frac{k_b \times T}{q} \quad (4)$$

$\mu(T)$ characterizes the electron mobility [36, 37] and is a function of temperature, its expression is given by:

$$\mu(T) = 1,43.10^9 T^{-2,42} cm^2 V^{-1} s^{-1} \quad (5)$$

k_b is the Boltzmann constant, q the elementary charge of the electron and T the temperature.

L^*(B, T) represents the diffusion length of the minority carriers of charges in the base and is given by:

$$L^*(T,B) = \sqrt{D^*(T,B).\tau} \quad (6)$$

τ is the lifetime of the minority charge carriers in the base.

δ (x, B, T) represents the density of minority carriers of charge in the base. It is obtained after the resolution of equation (1) and is given by:

$$\delta(x,B,T) = A.\cos\left(\frac{x}{L^*(B,T)}\right) + B.\sinh\left(\frac{x}{L^*(B,T)}\right) + \sum \frac{a_i.L^*(T,B)^2}{D^*(B,T).\left[L^*(B,T).b_i - 1\right]}.e^{-b_i.x} \quad (7)$$

The expressions of A and B are determined from the boundary conditions [38, 39]:

- at the junction(*x=0*)

$$\frac{\partial \delta(x,B,T)}{\partial x}\Big|_{x=0} = \frac{Sf.\delta(x,B,T)}{D(B,T)^*}\Big|_{x=0} \quad (8)$$

- at the back surface (*x=H*):

$$\frac{\partial \delta(x,B,T)}{\partial x}\Big|_{x=H} = -\frac{Sb.\delta(x,B,T)}{D(B,T)^*}\Big|_{x=H} \quad (9)$$

Sf represents the recombination velocity of the minority charge carriers at the junction. It characterizes the operating point of the solar cell but also the minority carrier flux at the junction [38,39]. Sb is the recombination velocity of the minority charge carriers at the back surface [39].

3. Results and Discussions

From equation 3, the profile of the diffusion coefficient as a function of temperature for different values of the magnetic field is shown in figure 2 [40].

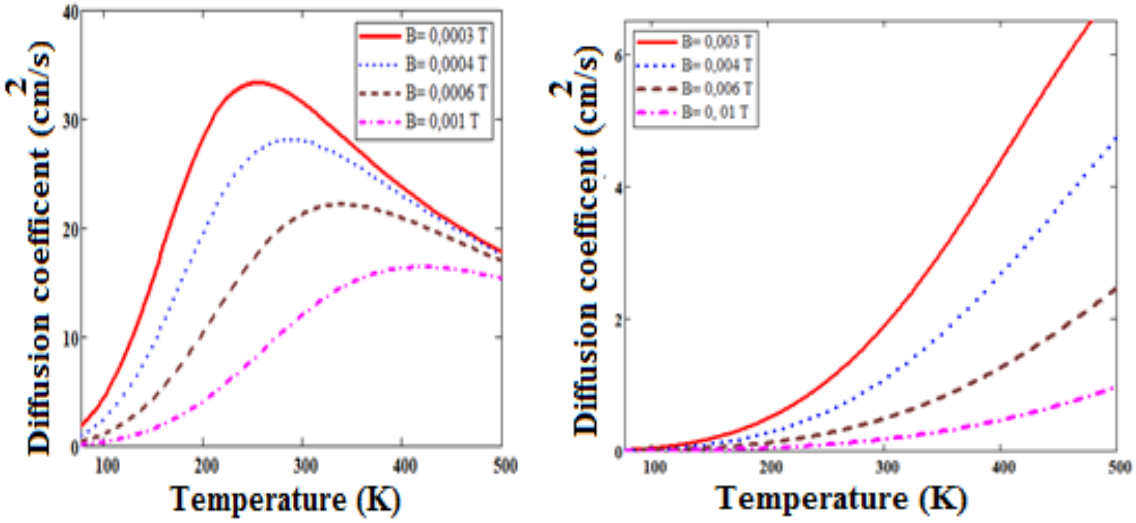

Figure 3: Diffusion coefficient as a function of temperature for different values of the magnetic field

The exploitation of figure 2 by the graphical method as well as by the analytical method made it possible to obtain Table 1 [40]:

Table 1: Variation of the amplitude of the diffusion coefficient as a function of the optimum temperature

Magnetic Field B (T)	**0.0003**	**0.0004**	**0.0005**	**0.0006**	**0.0007**	**0.0008**	**0.0009**	**0.001**
optimal temperature T (K)	255	285	308	335	355	380	400	410
Diffusion coefficient D (cm^2/s)	33.364	28.178	24.694	22.206	20.276	18.763	17.571	16.642

3.1. Study of the minority charge carriers density in excess in the base

From equation 7 and table 1, we represent in figure 3, the profile of the density of minority carriers as a function of the depth x for different optimum temperatures in a short-circuit situation.

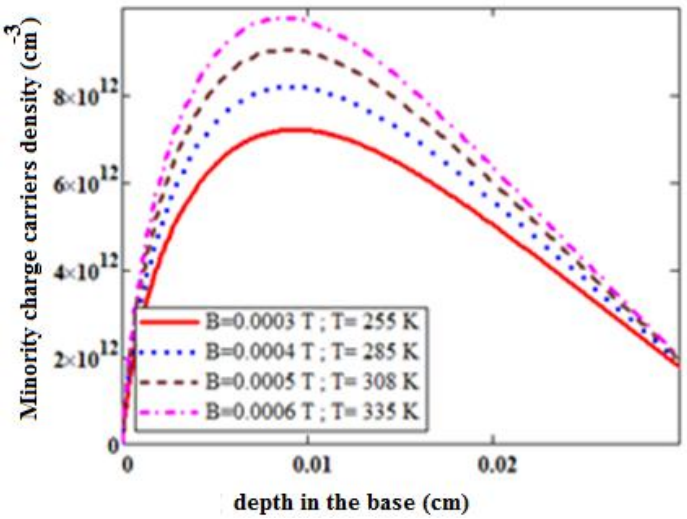

Figure 3: Minority charge carriers density as a function of the depth for different optimum temperatures, Sf=6.10^{6}cm/s

Figure 3 shows two essential observation areas:

- A first where the concentration gradient is positive. In this region the minority charge carriers cross the junction and participate in the photocurrent production.
- A second one where the concentration gradient is negative: it is a zone of predominance of the recombinations in volume of the minority carriers of charge because they lack energy enabling them to reach the junction and cross the potential barrier.

We also find that the maxima of the density of minority charge carriers increase with the optimal temperature. Indeed, the thermal agitation resulting from the rise in temperature reduces the mobility [41-43] and the maximum diffusion of the minority carriers from the base to the junction, which consequently leads to an increase in the density of minority carriers of load in the base [40]. In order to study the behavior of minority charge carriers when the solar cell is in the open circuit situation, we represent in Figure 4 the profile of the density of minority carriers as a function of the depth of the base for different optimum temperatures in open circuit

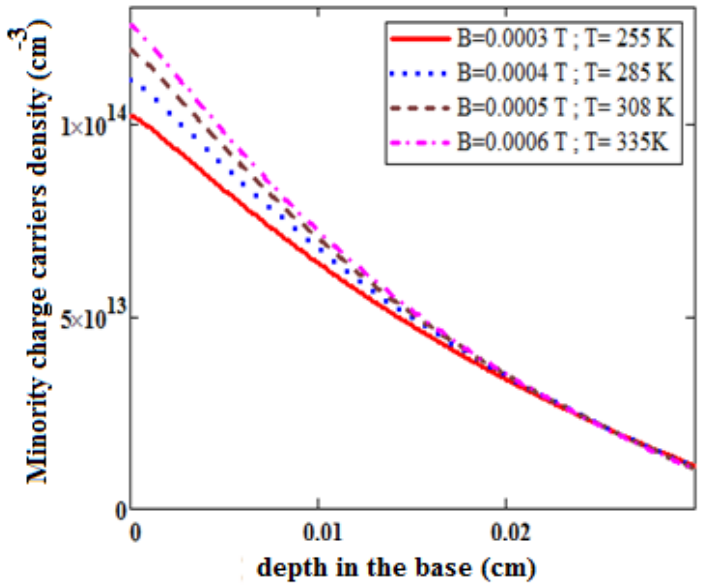

Figure 4: Minority charge carriers density as a function of the depth for different optimum temperatures in open circuit Sf=10 cm/s

For a given optimum temperature, figure 4 shows a decrease in the density of minority carriers with the increase in depth in the base. Indeed, going deep into the base, the photogeneration of the minority charge carriers decreases according to the equation 2 and given the low value of the recombination rate of the minority charge carriers at the junction, we inevitably witness a reduction of the charge carrier minority density.

Indeed, by going deep into the base, the photogeneration of the minority carriers of charge decreases according to equation 2 and given the low value of the recombination velocity of the minority carriers of charge at the junction, we inevitably to a reduction in the density of minority charge carriers. This effect of optimal temperature is more sensitive near the junction. Indeed, the more the charge carriers are accumulated at the junction, the more perceptible the effect of the thermal agitation. The effect of the thermal agitation increases the possibilities of recombination of the minority charge carriers in volume or on the surface when the solar cell is in the open circuit situation. Thus, Auger recombinations become important [44] and lead to a reduction in photocurrent [45]. To study the effects of the magnetic field and of the temperature we represent in figure 5, the profile of the density of minority carriers as a function of the temperature for different magnetic fields is shown.

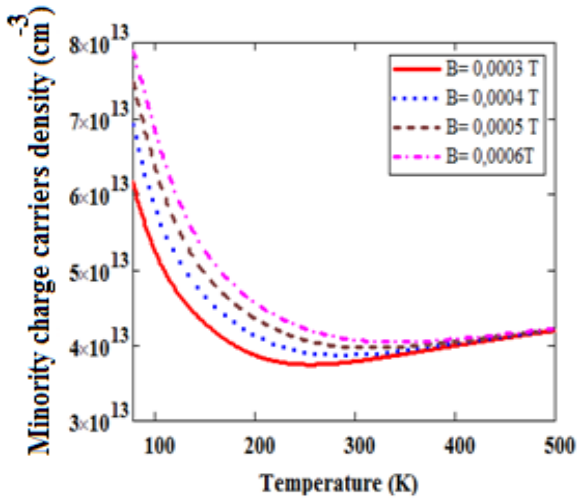

Figure 5: Minority charge carriers density as a function of the depth for different optimum temperatures Sf=3.10^3 cm/s, x=0.

Figure 5 shows that the density of minority carriers decreases until to a corresponding minimum value at a temperature called optimum temperature and then increases with temperature. Indeed, the decrease in the density of minority charge carriers for temperatures below the optimum temperature (T <Top (B)) is due to the increase of the low temperature thermal conductivity [46] in the semi- conductor according to the relationship of T^3 [47-49] and reduction of the thermal resistance of the material [48-50]: this is the normal process or N process [51, 52]. The increase of the density of minority carriers in excess with the temperature corresponds to the inverse effect, that is to say the high temperature situation (T> Top (B)) where the thermal conductivity decreases in the semiconductor material according to the relationship of 1 / T [47, 48, 50], whereas the thermal resistance of the material increases with the increase in temperature: this is the Umklapp process or U-shaped mechanism [48, 50, 53]. In the Umklapp process, two incident phonons with a sufficient wave vector give rise to a phonon of wavevector that exits the first Brillouin zone. This wave vector is brought back into the first Brillouin zone by a wave vector of the reciprocal lattice whose velocity is less than that of the sum of the incident wave vectors which in turn reduces the thermal conductivity [53] or temperatures above the optimum temperature (T>Top(B)). The minimum of minority carriers corresponds to a maximum diffusion of carriers from the base to the junction at a temperature equal to the optimal temperature (T=Top(B)). The latter delimits two physical processes, namely the Normal process which limits the thermal resistance [51,52] and the Umklapp process with limited thermal conductivity [51]. We also observe that the minimas of density of minority carriers increase with the magnetic field. Indeed, the increase in the magnetic field increases the optimum temperature and consequently reduces the possibilities of maximum diffusion of minority charge carriers in the base in order to generate a current to the external circuit [40].

3.2. Study of Photocurrent density

The expression of the photocurrent density is given by equation (10):

$$J_{Ph}(B,T) = q.D^{*}(B,T).\frac{\partial\delta(x,B,T)}{\partial x}\Big|_{x=0} \qquad (10)$$

From the relationship 10, we represent in figure 6 the profile of the photocurrent density as a function of the recombination velocity at the junction for different optimum temperatures.

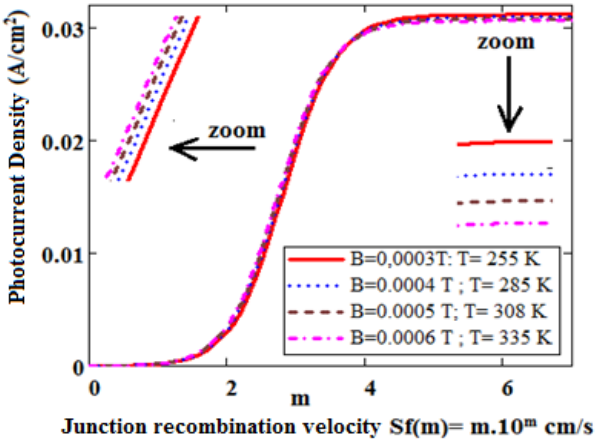

Figure 6: Photocurrent density as a function of the recombination velocity at the junction for different optimum temperatures

Figure 6 shows that at low values of the recombination velocity of the minority charge carriers at the junction (Sf) the photocurrent density is low and when this velocity tends towards its large values (near the short circuit), the photocurrent density increases to reach a maximum value: it is the photocurrent density of short circuit. Indeed, for the weak values of Sf, the minority charge carriers are blocked at the junction because they haven't enough energy to cross the junction. When Sf increases the minority charge carriers begins to cross the junction and the photocurrent increases. There is also an increase in the photocurrent density for an intermediate situation of the short circuit and open circuit. Indeed, temperature is a parameter whose variation leads to an abnormal change of the current [54]. Its elevation leads to the widening of the area of charge and space [55]. As a result, a significant number of minority charge carriers cross the junction to participate in the photocurrent. On the other hand, in the vicinity of the short-circuit, the increase of optimum temperature decreases the photocurrent. In order to better visualize the effects of temperature and magnetic field, we represent in figure 7 the profile of the photocurrent density as a function of the temperature for different magnetic fields.

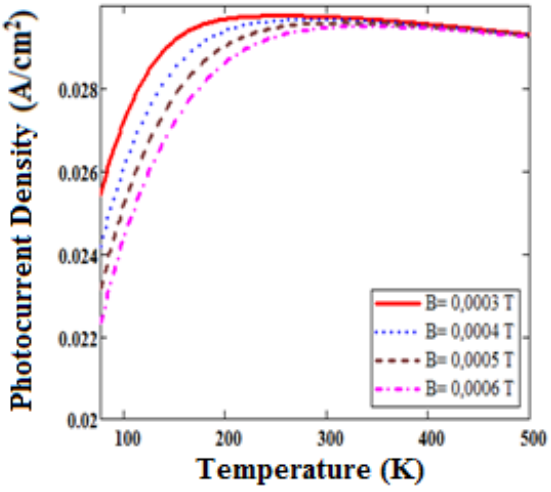

Figure 7: Photocurrent density as a function of the temperature for different magnetic fields. Sf=3.10³ cm/s.

La figure 7 shows a greater production of photocurrent at a temperature equal to the optimum temperature (T = Top (B)) for a given magnetic field. This is due to the beginning of the Umklapp process after an increase in the low-temperature thermal conductivity ie temperatures below the optimum temperature (T <Top (B)) [5] of the semiconductor material according to the relation T^3 [47-49]. Whereas, at high temperature, above the maximum thermal conductivity, the phonon-phonon interaction [46,52] or the umklapp process [48,50,53,54] predominates, thus reducing the thermal conductivity with the temperature rise [49,52] according to the 1 / T relationship [47,48,50], which results in reduced photocurrent production for temperatures above the optimum temperature. We also note that the photocurrent density decreases with the high values of the magnetic field. Indeed, the increase of the magnetic field is synonymous with the increase of the optimal temperature and consequently the reduction of the maximum diffusion of minority carriers in excess in the base [40]. Thus, at the figure 8, we represent the profile of the short-circuit photocurrent density as a function of the logarithm of the magnetic field for different optimum temperatures.

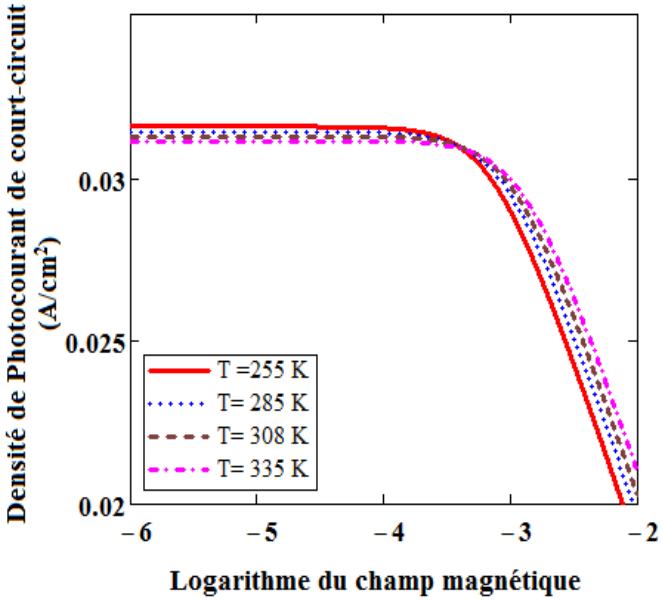

Figure 8: Short-circuit photocurrent density as a function of the logarithm of the magnetic field for different optimum temperatures

Figure 8 shows that at low values of the magnetic field, the short-circuit photocurrent is maximum and constant for a given optimum temperature. Here, the magnetic field has no effect on the diffusion of excess minority carriers. But beyond a magnetic field greater than 10^{-3}T, the short-circuit photocurrent decreases rapidly. Indeed, the magnetic field creates a magnetic force which deflects the photogenerated carriers from their initial trajectory towards the lateral surfaces, thus reducing their mobility, their diffusion and their conduction in the base [56].

4. Conclusion

In this work, the optimal temperature Topt (B) effect on the minority charge carriers density of excess carriers in the base and the photocurrent density is proposed. Study shows that the minority charge carriers density increases with the optimum temperature as well as with the magnetic field.

Moreover, the photocurrent density and the short-circuit current are maximum at an optimum temperature (T = Top (B)) and for a given magnetic field because of the maximum diffusion at this temperature, where neither the normal process nor the Umklapp process predominates.

References

[1]. Jakubowicz, A. (1980) Theory of lifetime measurements in thin semiconductor layers with the scanning electron microscope; transient analysis. *Solid-State Electronics*, 23, 635-639.

[2]. Saritas, M. and Mckell, H. D. (1988) Comparison of Minority carrier Diffusion Length Measurements in Silicon by the Photoconductive Decay and Surface Photo Voltage Methods. *Journal of Applied Physics*, 63, 4561- 4567.

[3]. Zerbo, I., Zougrana, M., Sourabie, I., Ouedraogo, A., Zouma, B., Bathiebo, D.J. (2015) External Magnetic Field Effect on Bifacial Silicon Solar Cell's Electric Power and Conversion Efficiency. *Turkish Journal of Physics*, 39, 288 – 294.

[4]. Sow, O., Zerbo, I., Mbodji, S., Ngom, M. I., Diouf, M. S., Sissoko, G. (2012) Silicon Solar Cell Under Electromagnetic Waves In Steady State: Electrical Parameters Determination Using The I-V And P-V Characteristics. *International Journal of Science, Environment and Technology*, 1, N^0 4, 230 – 246.

[5]. Jayashree, B., Ramani, Radhakrishna, M.C., Agrawal, A., Khan, S. A., Meulenberg, A. (2006) The Influence of High-Energy Lithium Ion Irradiation on Electrical Characteristics of Silicon and GaAs Solar Cells Final Version to be published. *IEEE Transactions on Nuclear Science*, 53, N° 6,1-8.

[6]. Sissoko, G. and Mbodji, S. (2011) A Method to Determine the Solar Cell Resistances from Single I-V Characteristic Curve Considering the Junction Recombination Velocity (Sf). *International Journal of Pure and Applied Sciences and Technology*, 6,103-114.

[7]. Charles, J.P., Haddi, A., Maouad, A., Bakhtiar, H., Zerga, A., Hoffmann, A., Mialhe, P. (2000) La Jonction du Solaire à la Microélectronique. *Revue des Energies Renouvelables*,3, 1-16.

[8]. Benmoussa, W.C., Amara, S. etZerga, A. (2007) Etude comparative des modèles de la caractéristiquecourant-tension d'une cellule solaire au silicium monocristallin. *Revue des Energies Renouvelables ICRESD*-07*Tlemcen, 301 – 306.*

[9]. Kumari, J. S. and Babu C.S. (2012) Mathematical Modeling and Simulation of Photovoltaic Cell Using Matlab-Simulink Environment. *International Journal of Electrical and Computer Engineering (IJECE)*, 2, 26-34.

[10]. Kowalczewski, P., Redorici, L., Bozzola, A., Andreani, L.C. (2016) Silicon Solar Cells Reaching the Efficiency Limits: from Simple to Complex Modeling. *Journal of Optics*, 18, 1-11.

[11]. Ngom, M.I., Zouma, B., Zoungrana, M., Thiame, M., Bako, Z. N., Camara, A. G., Sissoko, G. (2012) Theoretical Study of a Parallel Vertical Multi-Junction Silicon Cell under Multispectral Illumination: Influence of External Magnetic Field on the Electrical Parameters. *International Journal of Advanced Technology & Engineering Research*, 2, 101-109.

[12]. Faye, K., Gaye, I., Gueye, S., Wade, M. and Sissoko, G. (2014) Silicon Solar Cell under Back Side Illumination: Effect of Magnetic Field. *IPASJ-International Journal of Electrical Engineering (IIJEE)*, 2, 1-9.

[13]. Zoungrana, M., Dieng, B., Lemrabott, O.H., Toure, F., Moujtaba, M.A. O., Sow, M.L., Sissoko, G.(2012) External Electric Field Influence on Charge Carriers and Electrical Parameters of Polycrystalline Silicon Solar Cell. *Research Journal of Applied Sciences, Engineering and Technology* 4, 2967-2972.

[14]. Cheikh, M. L. O., Seibou, B., Moujtaba, M.A.O., Faye, K., Wade, M., Sissoko, G. (2015). Study of Base Doping Rate Effect on Parallel Vertical Junction Silicon Solar Cell under Magnetic Field. *International Journal of Engineering Trends and Technology*, 19, *44-55*.

[15]. Khelfaoui, F. and Remram M. (2000) Fonctionnement à Haute Température d'une Cellule Solaire à Base du Silicium Polycristallin. *Revuesdes EnergiesRenouvelables: Chemss*, 83-89.

[16]. Dieme, N., Zoungrana, M., Mbodji, S., Diallo, H.L., Ndiaye, M., Barro, F.I. and Sissoko,G. (2014). Influence of Temperature on the Electrical Parameters of Vertical Parallel Junction Silicon Solar Cell under Polychromatic Illumination in Steady State. *Research Journal of Applied Sciences, Engineering and Technology*, 7, 2559-2562.

[17]. Zoungrana, M., Zerbo, I., Barro, F.I., Sam, R., Touré, F., Samb, M.L. and Zougmoré, F. (2011) Modélisation à 3-D de l'influence de la taille des grains et de la vitesse de recombinaison aux joints de grain sur une photopile au silicium poly cristallin sous éclairement concentré. *Revue des Energies Renouvelables*, 14, 649 – 664.

[18]. Samb, M. L., Zoungrana, M., Sam, R., Dione, M. M., Deme,M. M. and Sissoko, G. (2010). Etude enModélisation à 3-D d'une Photopile au Silicium en Régime Statique Placée dans un ChampMagnétique et sous Eclairement Multi Spectral: Détermination des Paramètres Electriques. *Journal des Sciences*, 10, 23 – 38.

[19]. Toure, F., Zoungrana, M., Zouma, B., Mbodji, S., Gueye, S., Diao, A. and Sissoko, G. (2012) Influence of Magnetic Field on Electrical Model and Electrical Parameters of a Solar Cell Under Intense Multispectral Illumination. *Global Journal of Science Frontier Research Physics and Space Sciences*, 12, 50-59.

[20]. Nzonzolo, D., Lilonga-Boyenga, Sissoko, G. (2014) Illumination Level Effects on Macroscopic Parameters of a Bifacial Solar Cell. *Energy and Power Engineering*, 6, 25-36.

[21]. Shaltout, M.A. M., El-Nicklawy, M.M., Hassan, A.F., Rahoma, U.A., Sabry, M. (2000). The Temperature Dependence of the Spectral and Efficiency Behavior of Si Solar Cell Under Low Concentrated Solar Radiation, *Renewable Energy*, 21, 445-458.

[22]. Ly, I., Lemrabott, O.H., Dieng, B., Gaye, I., Gueye, S., Diouf, M.S. and Sissoko, G. (2012) Techniques de Détermination des Paramètres de Recombinaison et le Domaine de leur validité d'une Photopile Bifaciale au Silicium Polycristallin sous Eclairement Multi Spectral Constant en Régime Statique. *Revue des Energies Renouvelables*,15, 187-206.

[23]. BA, H.Y., Seibou, B., Gaye, I., LY, I. and Sissoko, G. (2014) Recombination Parameters Measurement of Silicon Solar Cell Under Constant White Bias Light With Incident Angle Current. *Trends in Technology and Sciences*, 3,411-415.

[24]. Culea, G. (2006) B'augmentation de L'efficacité Energétiquue des Panneaux Solaires par Orientation Dynamique the Sixth World Energy System. *Conference, Torino, Italy,* July 10-12, 377-380.

[25]. Lemrabolt, O. H,Ly, I.,Maiga, A. S., Wereme, A., Barro, F. I. and Sissoko, G. (2008) Bulk and Surface Recombination Parameters Measurement in Silicon Double Sided Solar Cell under Constant Monochromatic. *Journal des sciences.* 8, 44 –50.

[26]. Zerbo, I., Koalaga, Z., Barro, F. I., Zougmore, F., Ndiaye, A.L., Diao, A. and Sissoko, G. (2004). Silicon Solar Cell Recombination Parameters Determination Under Frequency Modulation White Light Using Short Circuit Current Phase. *Journal desSciences*, 4, 42-46.

[27]. Cisse, S., Ehemba, A. K., Mbow, B., Diallo, D., Wade, I. (2016) Study of the Influence of Irradiation on Parameters Electrical of Monofacial Solar Cell Containing Thin Film CIGS Under Illumination Monochromatic in Dynamic Frequency Mode. *Global Journal of Engineering Science and Research Management*, 3, 23-29.

[28]. Gaye, I., Sam, R., Seré, A.D., Barro, I.F Moujtaba, M.A.O., Mané, R. and Sissoko, G. (2012) Effect of Irradiation on Transient Response of Silicon Solar Cell. *International Journal of Emerging Trends Technology in Computer Science (IJETCS*), 1, 210-214.

[29]. Sumita, T., Imaizumi, M., Matsuda, S., Ohshima, T., Ohi, A., Itoh, H. (2003) Proton radiation analysis of multi-junction space solar cells. *Nuclear Instruments and Methods in Physics Research*, B 206, 448–451.

[30]. Diasse, O., Sam, R. S., Diallo, H. Ly., Ndiaye, M., Thiam, N., Mbodji S. and Sissoko, G. (2012) Solar cell's classification by the determination of the specific values of the back surface recombination velocities in open circuit and short-circuit operating conditions. *International Journal of Emerging Trends & Technology in Computer Science (IJETTCS),* 1, 55-59.

[31]. Ndiaye, M., Bako, Z. N., Zerbo, I., Dieng, A., Barro, F. I. and Sissoko, G. (2008). Détermination des Paramètres Electriques d'une Photopile Sous Eclairement Monochromatique en Modulation de Fréquence à Partir des Diagrammes de Bode et de Nyquist. *Journal des Sciences*, 8,59-68.

[32]. Mohamed, H.A. (2014) Theoretical Study of the Efficiency of CdS/PbS Thin Film Solar Cells. *Solar Energy*, 108, 360-369. www.elsevier.com/locate/solener.

[33]. Dione, M.M., Diallo, H. L., Wade, M., Ly, I., Thiame, M., Toure, F., Camara, A. G., Dieme, N., Bako, Z. N., Mbodji, S., Barro, F.I., Sissoko, G. (2011) Determination of the Shunt and Series Resistances of

a Vertical Multijunction SolarCell under Constant Multispectral Light. *Proceedings of the 26th European Photovoltaic Solar Energy Conference and Exhibition, Hamburg, Germany*, 250- 254.

[34]. Sudeepika, P., Khan, G. G., (2014). Analysis of Mathematical Model of PV Cell Module in Matlab/Simulink Environment. *International Journal of Advanced Research in Electrical, Electronics and Instrumentation Engineering*, 3, 7823-7829.

[35]. Said, S., Massoud, A., Benammar, M., Shehab A. (2012). A Matlab/Simulink-Based Photovoltaic Array Model Employing Sim Power Systems Toolbox. *Journal of Energy and Power Engineering*, 6, 1965-1975.

[36]. Kunst, M. and Sanders, A. (1992). Transport of Excess Carriers in Silicon Wafers. *Semiconductor Science and Technology*, 7, 51-59.

[37]. D. K. Schroder, J.D. Whitfield, and C. J. Varker. (1984). Recombination Lifetime using the Pulsed MOS Capacitor. IEEE Transactions on Electron Devices, 31, pp. 462-467.

[38]. H.L. Diallo, A. S. Maiga, A. Wereme, and G. Sissoko (2008). New approach of both junction and back surface recombination velocities in a 3D modelling study of a polycrystalline silicon solar cell. Eur. Phys. J. Appl. Phys. 42, pp: 203–211.

[39]. G. Sissoko, C. Museruka, A. Corréa, I. Gaye, A. L. Ndiaye. (1996). Light spectral effect on recombination parameters of silicon solar cell. World Renewable Energy Congress 3, Denver-USA pp. 1487-1490.

[40]. Mane, R., Ly, I., Wade, M., Datta, I., Diouf, M.S., Traore, Y., Ndiaye, M., Tamba, S., Sissoko, G. (2017) Minority Carrier Diffusion Coefficient *D**(*B*, *T*): Study in Temperature on Silicon Solar Cell under Magnetic Field. *Energy and Power Engineering*, 9, 1-10.

[41]. Sari-Ali, I., Benyoucef, B. and Chikh-Bled, B. (2007) Etude de la Jonction d'un Semi-Conducteur a l'Equilibre Thermodynamique. *Journal of Electron Devices*, 5, 122-126.

[42]. Boukhatem, M.H., Tahchi, M., Mialhe, P. (2012) Determination of Carrier Temperature From Junction I(V) Measurements. *Journal of Electron Devices*, 15, 1269 -1273.

[43]. Streetman, B. G., and Banerjee, S. K. (2006). Solid State Electronic Devices, 6th ed. Upper Saddle River, NJ: Prentice Hall.

[44]. TiedjeI, T., Yablonovitch, E., Cody, G. D. and Brooks, B.G. (1984). Limiting Efficiency of Silicon Solar Cells. *IEEE Transactions on Electron Devices, ED*-31, N°5, 711-716.

[45]. Bernardi, M. (2016). First-principles dynamics of electrons and phonons. *The European Physical Journal B*, 89, 1-15.

[46]. Kim, P., Shi, L., Majumdar, A. and McEuen, P. L. (2001). Thermal Transport Measurements of Individual Multiwalled Nanotubes. *Physical Review Letters*, 87, 1-4.

[47]. Ferizović, D., Hussey, L.K., Huang, Y.S. and Muñoz, M. (2009). Determination of the Room Temperature Thermal Conductivity of RuO_2 by the Photothermal Deflection Technique. *Applied Physics Letters*, 94, 1-3.

[48]. Berman, R. (1951) Thermal Conductivity of Dielectric Crystals: The "Umklapp". Nature, 168, 277-280.

[49]. McConnell, A. D., Uma, S., Goodson, K. E. (2001) Thermal Conductivity of Doped Polysilicon Layers. *Journal of Microelectromechanical Systems*, 10, N° 3, 360-369.

[50]. Casimir, H.B.G. (1938) Note on the Conduction of Heat in Crystals. *Physica*, 5, 495-500.

[51]. Guillou, G.L., Albany, H.J. (1970) Contribution des Phonons Transverses et Longitudinaux à la Conductivité Thermique de Réseau de l'Antimoniure de Galium à Basse Température. *Journal de Physique*, Tome 31, N°5-6, 495- 500.

[52]. Ghosh, S., Bao, W., Nika, D. L., Subrina, S., Pokatilov, E.P., Lau, C.N. and Balandin, A.A. (2010). Dimensional Crossover of Thermal Transport in Few-layer Graphene. *Nature Materiels*, 9, 555-558. www.nature.com/naturematerials

[53]. Freitag, M., Steiner, M., Martin, Y., Perebeinos, V., Chen, Z., Tsang, J.C. and Avouris, P. (2009) Energy Dissipation in Graphene Field-Effect Transistors. *Nano Letters*, 9, 1883-1888.

[54]. Sadiqa, A. A., Naseem, B. S., Iqbal, F. (2013) Fabrication Possibilities Source LDrainSchottkyFets Using Wet Chemical Technique on p-type (100) Silicon. *Journal of Electron Devices*, 17, 1406-1411.

[55]. Peet, M. J., Hasan, H. S. and Bhadeshia, H. K. D. H. (2011) Prediction of Thermal Conductivity of Steel. *International Journal of Heat and Mass Transfer*, 54, 2602-2608.

[56]. Diao, A., Thiam, N., Zoungrana, M., Sahin, G., Ndiaye, M. and Sissoko, G. (2014) Diffusion Coefficient in Silicon Solar Cell with Applied Magnetic Field and under Frequency: Electric Equivalent Circuits. *World Journal of Condensed Matter Physics*, 4, 84-92.